

Manifolds.jl: An Extensible Julia Framework for Data Analysis on Manifolds

Seth D. Axen

SETH.AXEN@GMAIL.COM

*Cluster of Excellence Machine Learning: New Perspectives for Science
University of Tübingen
Maria-von-Linden-Str. 6, 72076 Tübingen, Germany*

Mateusz Baran

MBARAN@AGH.EDU.PL

*AGH University of Science and Technology
30 Mickiewicz Ave., 30-059 Krakow, Poland*

*Cracow University of Technology
Faculty of Materials Science and Physics
Podchorążych 1, 30-084 Krakow, Poland*

Ronny Bergmann

RONNY.BERGMANN@NTNU.NO

*Department of Mathematical Sciences
Norwegian University of Science and Technology
NO-7041 Trondheim, Norway*

Krzysztof Rzecki

KRZ@AGH.EDU.PL

*AGH University of Science and Technology
30 Mickiewicz Ave., 30-059 Krakow, Poland*

*Cracow University of Technology
Faculty of Materials Science and Physics
Podchorążych 1, 30-084 Krakow, Poland*

Abstract

For data given on a nonlinear space, like angles, symmetric positive matrices, the sphere, or the hyperbolic space, there is often enough structure to form a Riemannian manifold. We present the Julia package `Manifolds.jl`, providing a fast and easy to use library of Riemannian manifolds and Lie groups. We introduce a common interface, available in `ManifoldsBase.jl`, with which new manifolds, applications, and algorithms can be implemented. We demonstrate the utility of `Manifolds.jl` using Bézier splines, an optimization task on manifolds, and a principal component analysis on nonlinear data. In a benchmark, `Manifolds.jl` outperforms existing packages in Matlab or Python by several orders of magnitude and is about twice as fast as a comparable package implemented in C++.

Keywords: Riemannian manifold, Lie group, nonlinear spaces, exponential map, logarithmic map, Julia, scientific computing, optimization on manifolds

1. Introduction

Data with a nonlinear structure appear in many applications. Addition or multiplication of such data by scalars may require disregarding the data's intrinsic structure. This complicates data analysis, as many analyses, such as computation of the mean, assume these are valid

operations. However, with enough properties (or, mathematically speaking, structure), such a space of nonlinear data is a Riemannian manifold, or manifold for short. Using tools of differential geometry, many operations can be generalized to manifolds by using only these generic properties. One example is the Riemannian center of mass (Grove and Karcher, 1973; Karcher, 1977), which generalizes the classical, Euclidean mean. Closed-form expressions for these operations do not always exist, but efficient implementations to approximate them are still often possible. Recent advances continue to resolve numerical challenges with efficiently implementing these operations. This makes data analysis for manifold-valued data more accessible.

Nonlinear data appears in many applications. The manifold of symmetric positive definite matrices (SPD) is used in diffusion tensor imaging (Dryden et al., 2009; Ghosh et al., 2008), the special orthogonal group of rotations is used in analysis of data from orientation sensors (Marins et al., 2001), and the sphere is used in various applications of directional statistics such as hydrology (Chen et al., 2013). The discipline of computational anatomy (Grenander and Miller, 1998; Cruz-Orive et al., 1985) extensively uses geometric methods, including Large Deformation Diffeomorphic Metric Mapping (Miller, 2004) with applications to medical data analysis (Pennec et al., 2019; Tulik et al., 2019). In image analysis, Grassmann and Stiefel manifolds are used for pose estimation by Turaga et al. (2011). Various manifolds with Fisher-Rao-like metrics are also used for shape analysis by, for example, Srivastava et al. (2011), Baran (2018), and Rzecki and Baran (2021).

A key obstacle to wider adoption of geometric methods is lack of a common, extensible, and efficient collection of operations on manifolds. One of the first toolboxes for optimization tools on manifolds was the Matlab package Manopt (Boumal et al., 2014). Several libraries followed, such as the C++ library ROPTLIB (Huang et al., 2018). The five major libraries for differential geometry in Python are Pymanopt (Townsend et al., 2016), Geomstats (Miolane et al., 2020), Geoopt (Kochurov et al., 2020), TheanoGeometry (Kühnel and Sommer, 2017), and McTorch (Meghwanshi et al., 2018), each with their own implementations of manifolds. Some libraries are more focused on specific tasks. For example, MVIRT (Bergmann, 2017) provides a variational model formulation for manifold-valued image processing. This toolbox introduces implementations of a cyclic proximal point algorithm (Bačák, 2014) applied to first- and second-order total variation (Bačák et al., 2016), as well as total generalized variation (Bergmann et al., 2018). MVIRT also provides the parallel Douglas–Rachford algorithm (Bergmann et al., 2016) for large-scale nonsmooth optimization.

The above packages all follow the same approach to generically implement their statistical or optimization algorithms for an arbitrary Riemannian manifold and provide a certain set of Riemannian manifolds that use this generic implementation. The speed of an algorithm then depends on efficiency of both the abstract implementation of the algorithm as well as of employed operations on the specific manifold considered in an application.

Here we present the Julia package `Manifolds.jl`, together with its accompanying interface package `ManifoldsBase.jl`. They provide an easily extensible interface to implement methods on a generic Riemannian manifold. Moreover, they implement a comprehensive, well-documented library of efficient implementations of operations on existing manifolds.

The remainder of this paper is organized as follows: Section 2 provides basic definitions of concepts from differential geometry and illustrates them using the unit sphere. Next,

Section 3 describes the general design of `Manifolds.jl`. Section 4 compares features of this library to what other libraries offer. A few examples of usage of `Manifolds.jl` are given in Section 5. Section 6 presents performance benchmarks of `Manifolds.jl` and other libraries on a set of manifolds for selected operations. Finally, conclusions are contained in Section 7.

2. Manifolds

In this section, relevant concepts from differential geometry are introduced. After introducing manifolds and related terms and definitions, the concepts are illustrated using the unit sphere in \mathbb{R}^3 in Section 2.2.

2.1 General definitions

Informally, a d -dimensional Riemannian manifold is defined as a set \mathcal{M} covered with a suitable collection of charts $\phi: U \rightarrow \mathbb{R}^d$ that locally identify open subsets $U \subset \mathcal{M}$ of \mathcal{M} with open subsets of \mathbb{R}^d . The most prominent property of this collection of charts, called an atlas of the manifold, is that each transition map $\varphi \circ \psi^{-1}: \mathbb{R}^d \rightarrow \mathbb{R}^d$ from one chart ϕ to another chart ψ is smooth. One way to work on manifolds is to work in charts. Any points $p, q \in U$ can be connected by a path using the chart. However, for general $p, q \in \mathcal{M}$, where the points are not in the domain of the same chart, then it is necessary to track a chain of charts along the path with transition maps between the charts to connect them. Intrinsic methods are independent from the actual choice of chart(s). For example, the distance or shortest path between two points should be independent of the choice of chart(s). Often it is more computationally convenient to represent points on a manifold using coordinates of an embedding, instead of using a chart.

On a d -dimensional manifold \mathcal{M} , we can define a curve $c(t)$, $c: I \supset [0, 1] \rightarrow \mathcal{M}$ and investigate its derivative $\dot{c}(t)$, whose values are analogous to the velocity of $c(t)$. For a fixed number $t_0 \in I$ and a chart ϕ that covers a neighborhood of $c(t_0) \in \mathcal{M}$, the function $t \mapsto \phi(c(t))$ is the corresponding curve in the chart, i.e. on \mathbb{R}^d . Note that different curves c_1, c_2 might have the same derivative at a point, $\dot{c}_1(t_0) = \dot{c}_2(t_0) = V$. We introduce the equivalence class of all such curves with the same derivative V . The collection of derivatives of all differentiable curves at some point $p \in \mathcal{M}$ under this equivalence class is the tangent space $T_p\mathcal{M}$; $T_p\mathcal{M}$ is a d -dimensional vector space at each point p on the manifold \mathcal{M} . The collection of all tangent spaces is called the tangent bundle $T\mathcal{M}$. On the tangent bundle, we can define a vector field as the map $V: \mathcal{M} \rightarrow T\mathcal{M}$, which assigns to each point a vector in its tangent space $V(p) \in T_p\mathcal{M}$.

These vector fields can be used to state the next two important tools: the Riemannian metric and connections. While a metric equips a manifold with notions of speed, distance, and angles, the connection relates tangent vectors from tangent spaces at different points.

A Riemannian metric is a function that maps any two tangent vectors at each point $p \in \mathcal{M}$ to a real number, $\langle \cdot, \cdot \rangle_p: T_p\mathcal{M} \times T_p\mathcal{M} \rightarrow \mathbb{R}$. For any p , the metric $\langle \cdot, \cdot \rangle_p$ is symmetric and linear in both of its arguments and positive definite. For two smooth tangent vector fields $V, W: \mathcal{M} \rightarrow T\mathcal{M}$, where $V(p), W(p) \in T_p\mathcal{M}$, the function $p \mapsto \langle V(p), W(p) \rangle_p$ is smooth. In this sense, the Riemannian metric is smooth in p . Note that the metric is a family of inner products with the additional property of being smooth in p . Like the inner product in \mathbb{R}^d , the output of the metric for two unit tangent vectors is $\cos \theta$, where θ is the angle between

the vectors. Moreover, the metric induces a vector norm on the tangent space. For a smooth function $f: \mathcal{M} \rightarrow \mathbb{R}$, the metric provides the notion of a gradient $\text{grad } f$, which informally is the direction of steepest ascent of f . While we have described the metric for real manifolds, `Manifolds.jl` can also represent metrics for complex and quaternionic manifolds.

A connection is a notion of taking the derivative of a vector field V along a curve $c(t)$. This tool enables to define higher order derivatives, such as the Hessian matrix of second-order derivatives of the function f from above. Acceleration-free curves are called geodesics. They generalize the concept of a straight line on a manifold, but more than one geodesic may join two points. The length of a shortest geodesic between two points enables us to compute the intrinsic distance between the points on the manifold.

There are several useful maps between a manifold and its tangent bundle. For a point $p \in \mathcal{M}$ and a direction $X \in T_p\mathcal{M}$ with length $\|X\|_p = \sqrt{\langle X, X \rangle_p}$, the geodesic starting at p with velocity X is locally uniquely determined. The value of the exponential map $\exp_p: T_p\mathcal{M} \supseteq W \rightarrow \mathcal{M}$ for the tangent vector X is the point $q = \exp_p(tX)$ this geodesic reaches at $t = 1$. The exponential map, in general, may only be defined for a subset W of the tangent space. The inverse of the exponential map, which yields the tangent vector X , is called the logarithmic map $\exp_p^{-1} = \log_p: q = \exp_p X \mapsto X$, and may be defined on only a subset of the image of the exponential map.

In some cases, the exponential and logarithmic maps can be derived in closed form, but otherwise they are expensive to evaluate. Therefore, one often uses a retraction $\text{retr}_p: T_p\mathcal{M} \rightarrow \mathcal{M}$, which approximates the exponential map. When the retraction can be inverted, i.e. from p and q we obtain X , this inverse retraction $\text{retr}_p^{-1}: q = \text{retr}_p X \mapsto X$ can be used to approximate the logarithmic map.

Finally, since tangent vectors $X \in T_p\mathcal{M}$ are defined only at their associated point p , there is a need to “transport” X to another point, say $q \in \mathcal{M}$. This can be done by the so-called parallel transport $\text{PT}_{q \leftarrow p} X$. Because this map is roughly as expensive to compute as the geodesic, it is often approximated with other methods, called vector transports.

For more details we refer to the textbooks (Absil et al., 2008; do Carmo, 1992).

2.2 Example: the two-dimensional unit sphere

The unit sphere in the three-dimensional Euclidean space, denoted \mathbb{S}^2 , is an intuitive example of a Riemannian manifold. Points on the unit sphere have unit norm. Adding (or subtracting) two of these points yields a point with a non-unit norm, which therefore does not belong to \mathbb{S}^2 . However, there is an intuitive way of reinterpreting subtraction that makes an analogous operation on the sphere possible.

We can interpret the difference $y - x$ between two points $x, y \in \mathbb{R}^3$ as a vector starting from x and pointing to y . Multiplying such a vector by a scalar and adding it to x defines a set of points on a straight line passing through x and y . This line segment joining x and y is the geodesic on \mathbb{R}^3 . On \mathbb{S}^2 , the shortest geodesic is no longer a line segment but is instead a shortest great arc passing through points $p, q \in \mathbb{S}^2$. For any two non-opposing points, the intersection of their common plane through the origin with the sphere yields two geodesics, one shorter than the other. We call this shorter great arc the shortest geodesic. For two opposing points $p, -p \in \mathbb{S}^2$, all great arcs that join the two points are half-circles; they are therefore joined by infinite shortest geodesics. We can measure the distance $d_{\mathbb{S}^2}(p, q)$

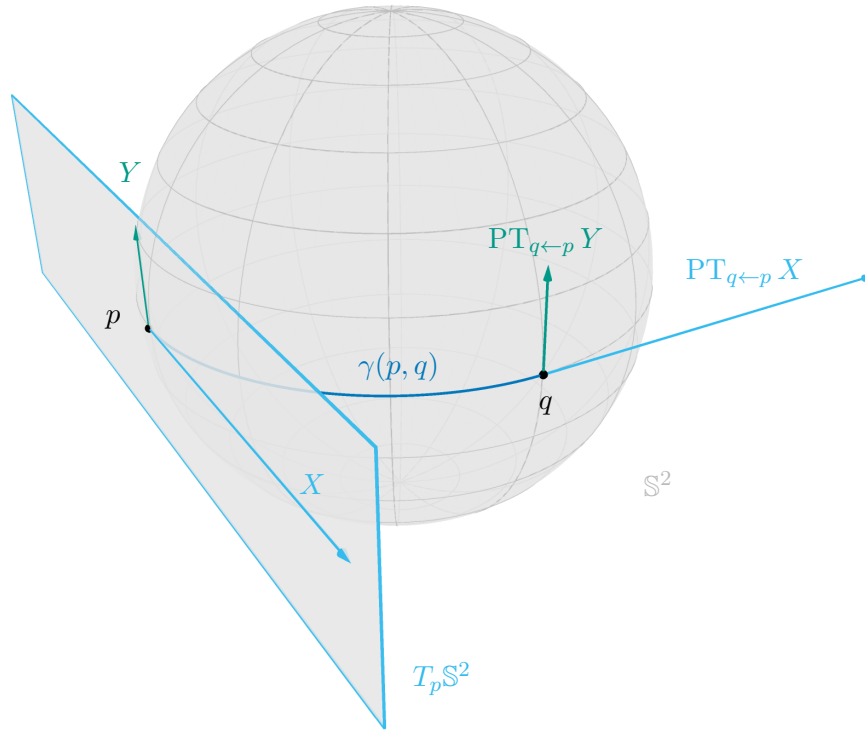


Figure 1: Unit sphere in \mathbb{R}^3 with two points p, q . Tangent space at p is labelled $T_p \mathbb{S}^2$, geodesic between p and q is the blue arc $\gamma(p, q)$ and the vector X is the tangent vector from $T_p \mathbb{S}^2$ that points towards q . Y is another vector from $T_p \mathbb{S}^2$ orthogonal to X . All tangent vectors are blue. Parallel transports of X and Y from p to q are shown as vector $PT_{q \leftarrow p} X$ and $PT_{q \leftarrow p} Y$, respectively.

between the points p and q as the length of a shortest geodesic, depicted as the blue curve in Figure 1.

If we draw a vector X tangent to the sphere at a point p , that is, tangent to some geodesic passing through p , this vector is in the tangent plane to \mathbb{S}^2 at p . If we choose X so that the motion along the shortest geodesic in the direction of X after a unit of time arrives at point q , then the logarithmic map $X = \log_p q$ computes X from p and q . The inverse function that takes a tangent vector X at a point p and tells at which point the vector is pointing is called the exponential map and is denoted $q = \exp_p X$.

Vectors tangent to the sphere at different points cannot be added or subtracted. First, they need to be transported to the same point. This is performed using parallel transport. Transport of a vector X tangent at p to a point q is denoted $PT_{q \leftarrow p} X$. This operation results in a new vector tangent to the sphere at q . Note that transporting a vector X tangent at p between a series of points, for example from p to q , from q to r and from r back to p , may not result in the same vector X .

These operations can be extended to all manifolds as described in Section 2.1.

3. Structure of the library

In this section we explore the basic structure of the library `Manifolds.jl` version 0.5.4 and its interface `ManifoldsBase.jl` version 0.11.4. We look at how to define a manifold, functions thereon, and extensions to manifolds using a decorator pattern.

3.1 Functions on manifolds

A new manifold in `Manifolds.jl` is defined by a struct `MyManifold{ \mathbb{F} } <: AbstractManifold{ \mathbb{F} }`, where \mathbb{F} is a parameter for the field the manifold is based on: the real numbers \mathbb{R} , complex numbers \mathbb{C} , or quaternions \mathbb{H} . Interface functions have both in-place and allocating versions. The allocating version allocates an output and then calls the in-place version, so a user only needs to implement the in-place version. For example, for the exponential map, the function `exp!(M, q, p, X)` must be implemented, which computes $\exp_p X$ in place of q . The allocating version `exp(M, p, X)` is then automatically available.

Usually there is no need to introduce types for points and vectors, unless different representations should be distinguished. For example, for the `Hyperbolic` manifold, the hyperboloid, Poincaré ball, and Poincaré half-space representations are implemented with only a few interface function overloads.

3.2 Features on manifolds using a decorator pattern

Using our interface, it is straightforward to implement a manifold with a default (i.e., implicit) metric. However, it is also possible to implement alternative metrics for the same manifold. In order to use a different metric, we define a type `MyMetric <: RiemannianMetric`. We can then equip our manifold with this new metric using the metric decorator type `MetricManifold{MyManifold, MyMetric}`. This can be used to implement a new inner product as well as all other functions affected by the metric, while leaving unchanged all functionality of `MyManifold` that are independent of the metric. For example, the manifold dimension is automatically available as well as checks for valid points or tangent vectors.

`MetricManifold` is one example of a decorator. Decorators can in general be used to equip an existing manifold with new or altered structure or functionality without requiring any changes to the type hierarchy. This is implemented using a traits-based approach.

Several additional decorators are implemented. The `EmbeddedManifold` introduces an embedding that submerges the manifold into another manifold. This provides the manifold with a projection from the manifold of the embedding onto the embedded manifold.

We can also equip a manifold with the structure of a Lie group using `GroupManifold`. For example, calling `GroupManifold(Euclidean(n), AdditionOperation())` equips the `Euclidean` manifold with the group operation of addition. As a result, points interpreted as group elements can be inverted using negation, translated via addition, and inverse translated via subtraction. The group logarithm and exponential are likewise simply addition and subtraction. As a result, no special overloads are needed for manifolds like `SymmetricMatrices` that can also be equipped with a group structure under addition. Similarly, an existing group can be equipped with a group structure under the operation of multiplication, along with suitable default implementations of group inversion, identity, translation, inverse translation, and the group exponential. For example, while `Rotations(n)` implements the manifold structure of

the special orthogonal group $SO(n)$, the manifold can be equipped with the group operation of multiplication by calling `GroupManifolds(Rotations(n), MultiplicationOperation())` or the useful alias `SpecialOrthogonal(n)`. We also introduce `AbstractGroupAction` to define the action of a group on another manifold. Two groups together with an action of one group on the other can be joined to form a `SemidirectProductGroup`, which is again just a convenient alias for a `GroupManifold`. A Riemannian metric defined on the Lie algebra of a group can be extended to the entire group using `InvariantMetric`.

The `ValidationManifold` overloads many functions to check that input and output points and tangent vectors of respective methods on the wrapped manifold are valid. This is useful for development of new manifolds and algorithms.

Another usage of the decorator pattern is the `AbstractEmbeddedManifold`. Here, the idea of `EmbeddedManifold` is reversed, in the sense that instead of first implementing a manifold and then specifying its embedding, the manifold is implemented with the help of the embedding. For example the `Sphere` can be implemented independently, but for the (default, round) metric, the inner product `inner(::Sphere, p, X, Y)` of two tangent vectors $X, Y \in T_p\mathcal{M}$ can also be computed using the inner product in the embedding. In other words, the Riemannian metric $\langle \cdot, \cdot \rangle_p$ on the sphere \mathbb{S}^{d-1} at a point p is the Euclidean metric $\langle \cdot, \cdot \rangle$ from the embedding \mathbb{R}^d restricted to the tangent plane $T_p\mathbb{S}^{d-1}$. The `AbstractEmbeddedManifold` has a parameter `AbstractEmbeddingType` to specify the type of embedding for the manifold one aims to implement. Defining a manifold to be `DefaultIsometricEmbeddingType` means, that the inner products are computed calling the inner product function of the embedding. The level can be increased to the `TransparentIsometricEmbedding`, where even the exponential and the logarithmic maps are computed by calling the corresponding functions for the embedding. This is for example the case for the `SymmetricMatrices(n)`, $n \in \mathbb{N}$ manifold, which are represented by their complete symmetric matrix, though this is redundant. Its exponential map is the addition of matrices and hence inherited from the space of matrices `Euclidean(n, n)`.

Similarly the `AbstractGroupManifold <: AbstractEmbeddedManifold` is available to implement a group manifold directly instead of equipping a given manifold with a group operation. Due to the inheritance, this can also be combined with the features given by an `AbstractEmbeddedManifold`.

4. Comparison to other libraries

Table 1 compares availability of manifolds in `Manifolds.jl` 0.5.4 to other existing libraries: `Geomstats` 2.2.3 (Miolane et al., 2020), `Geopt` 0.3.1 (Kochurov et al., 2020), `Manopt` 6.0 (Boumal et al., 2014), `McTorch` 1.1 (Meghwanshi et al., 2018), `Pymanopt` 0.2.5 (Townsend et al., 2016), `ROPTLIB` 0.8 (Huang et al., 2018), and `TheanoGeometry` (Kühnel and Sommer, 2017). Availability of different operations is compared in Table 2.

Note that the extent of support varies significantly across libraries. For example `Manifolds.jl` implements three different metrics on the manifold of symmetric positive definite matrices. On the other hand, `Geomstats` extensively tests compatibility with different automatic differentiation backends, while other libraries do so for a smaller set of operations.

Table 1: Comparison of manifolds available in related libraries. A manifold is considered to be available if at least a retraction is implemented using a generic interface. We denote by \mathbb{R} , \mathbb{C} , \mathbb{H} up to which type of field a manifold is available and with \times that the manifold is not available in a package.

^a this manifold is available for arrays with any number of indices.

Manifold	Geomstats	Geopt	Manifolds.jl	Manopt	McTorch	Pymanopt	ROPTLIB	TheanoGeometry
Centered matrices	\times	\times	\mathbb{C}	\mathbb{R}	\times	\times	\times	\mathbb{R}
Discretized curves	\mathbb{R}	\times	\times	\times	\times	\times	\times	\times
Elipsoid	\times	\times	\times	\times	\times	\times	\times	\mathbb{R}
Elliptope	\times	\times	\mathbb{R}	\mathbb{R}	\times	\times	\times	\times
Essential manifold	\times	\times	\mathbb{R}	\mathbb{R}	\times	\times	\times	\times
Euclidean	\mathbb{R}	\mathbb{R}	\mathbb{H}^a	\mathbb{C}	\mathbb{R}	\mathbb{R}	\mathbb{R}	\mathbb{R}
Fixed rank matrices	\times	\times	\mathbb{C}	\mathbb{R}	\times	\times	\mathbb{C}	\times
General linear group	\mathbb{R}	\times	\mathbb{C}	\times	\times	\times	\times	\mathbb{R}
Generalized Grassmann	\times	\times	\mathbb{C}	\mathbb{R}	\times	\times	\times	\times
Generalized Stiefel	\times	\times	\mathbb{C}	\mathbb{R}	\times	\times	\times	\times
Grassmann	\mathbb{R}	\times	\mathbb{C}	\mathbb{C}	\times	\mathbb{R}	\mathbb{R}	\times
Hilbert sphere	\times	\times	\times	\times	\times	\times	\mathbb{R}	\times
Hyperbolic space	\mathbb{R}	\mathbb{R}	\mathbb{R}	\mathbb{R}	\times	\times	\times	\times
Lorentzian manifold	\mathbb{R}	\mathbb{R}	\mathbb{R}	\times	\times	\times	\times	\times
Multinomial doubly stochastic matrices	\times	\mathbb{R}	\mathbb{R}	\mathbb{R}	\times	\times	\times	\times
Multinomial matrices	\times	\times	\mathbb{R}	\mathbb{R}	\times	\times	\times	\times
Multnomial symmetric matrices	\times	\times	\mathbb{R}	\mathbb{R}	\times	\times	\times	\times
Oblique manifold	\times	\times	\mathbb{R}	\mathbb{R}	\times	\mathbb{R}	\mathbb{R}	\times
Phases of real DFT	\times	\times	\times	\mathbb{C}	\times	\times	\times	\times
Positive numbers	\times	\times	\mathbb{R}	\mathbb{R}	\times	\mathbb{R}	\mathbb{R}	\times
Probability simplex	\mathbb{R}	\times	\mathbb{R}	\mathbb{R}	\times	\times	\times	\times
Product Space	\mathbb{R}	\mathbb{R}	\mathbb{H}	\mathbb{C}	\times	\mathbb{C}	\mathbb{C}	\times
Projective Space	\times	\times	\mathbb{H}^a	\times	\times	\times	\times	\times
Rotations	\mathbb{R}	\times	\mathbb{R}	\mathbb{R}	\times	\mathbb{R}	\mathbb{R}	\mathbb{R}
Skew-symmetric matrices	\mathbb{R}	\times	\mathbb{C}	\mathbb{R}	\times	\times	\times	\times
Special Euclidean group	\mathbb{R}	\times	\mathbb{R}	\mathbb{R}	\times	\times	\times	\times
Spectrahedron	\times	\times	\mathbb{R}	\mathbb{R}	\times	\times	\times	\times
Sphere / Circle	\mathbb{R}	\mathbb{R}	\mathbb{C}^a	\mathbb{C}^a	\times	\mathbb{C}^a	\times	\mathbb{R}
Stiefel	\mathbb{R}	\mathbb{R}	\mathbb{C}	\mathbb{C}	\mathbb{R}	\mathbb{R}	\mathbb{C}	\times
Sym. matrices	\mathbb{R}	\times	\mathbb{C}	\mathbb{R}	\times	\times	\times	\times
Sym. pos. def. matrices	\mathbb{R}	\times	\mathbb{R}	\mathbb{R}	\mathbb{R}	\mathbb{R}	\mathbb{R}	\mathbb{R}
Sym. pos. def. simplex	\times	\times	\times	\mathbb{C}	\times	\times	\times	\times
Sym. pos. semidef. fixed rank matrices	\times	\times	\mathbb{C}	\mathbb{C}	\times	\mathbb{C}	\mathbb{C}	\times
Unit-norm sym. matrices	\times	\times	\mathbb{C}	\mathbb{R}	\times	\times	\times	\times

Table 2: Comparison of features available in related libraries.

Feature	Geomstats	Geoopt	Manifolds.jl	Manopt	McTorch	Pymanopt	ROPTLIB	TheanoGeometry
Atlases and charts	✗	✗	✓	✗	✗	✗	✗	✗
Automatic differentiation	✓	✓	✓	✗	✓	✓	✗	✓
Compatibility with extended precision floating point types	✗	✗	✓	✓	✗	✗	✗	✗
Bases of tangent spaces	✗	✗	✓	✗	✗	✗	✗	✗
Connections	✓	✗	✗	✗	✗	✗	✗	✗
Exponential maps (retractions)	✓	✓	✓	✓	✓	✓	✓	✓
Inner product	✓	✓	✓	✓	✓	✓	✓	✓
Lie groups and actions	✓	✗	✓	✗	✗	✗	✗	✓
Logarithmic maps (inverse retractions)	✓	✓	✓	✓	✓	✓	✓	✓
Riemannian gradients	✗	✓	✓	✓	✓	✓	✓	✓
Riemannian Hessians	✗	✓	✗	✓	✓	✓	✓	✗
Vector transport	✓	✓	✓	✓	✓	✓	✓	✓

5. Examples

This section demonstrates a few examples of composing generic operations from `Manifolds.jl` with the Julia ecosystem (Bezanson et al., 2017). The first example defines a Bézier spline on a generic manifold to demonstrate how to easily define new functions on manifolds using `ManifoldsBase.jl`. Then, `Manopt.jl`¹ (Bergmann, 2019) is used as an example of a complex optimization library built on top of `Manifolds.jl`. Further, it is demonstrated how `Manifolds.jl` can be easily combined with independently developed libraries to implement fast, geometry-aware algorithms.

Note that all examples can be split into two components. First, a manifold and data on the manifolds are constructed. Second, the algorithm is executed on this manifold. Since all methods are implemented in a generic way, switching to data from another manifold just requires to change the first part of introducing the manifold and loading/generating corresponding data.

5.1 Implementing functions on manifolds

Functions on manifolds dispatch on the manifold itself, which is included as the first argument. As an example, we implement a Bézier curve on an arbitrary manifold. Bézier curves are used to model curves and surfaces in computer graphics. Their shape is determined by so called control points. The curve starts in the first control point and ends in the last. For more details on their use on manifolds, see for example (Absil et al., 2016; Gousenbourger et al., 2018; Bergmann and Gousenbourger, 2018).

A Bézier curve can be defined using the De Casteljau algorithm. Let us first consider the classical Euclidean case: given a degree n and $n + 1$ (control) points $x_0, \dots, x_n \in \mathbb{R}^n$,

1. Current version 0.3.9, available at <https://manoptjl.org>

the Bézier curve $b_n(t; x_0, \dots, x_n)$ is defined recursively as

$$\begin{aligned} b_n(t; x_0, \dots, x_n) &= b_1(t; b_{n-1}(t; x_0, \dots, x_{n-1}), b_{n-1}(t; x_1, \dots, x_n)) \\ b_1(t; x_0, x_1) &= x_0 + t(x_1 - x_0) \end{aligned}$$

A Bézier curve $b_1(t; x_0, x_1)$ of order 1 is just a line. To evaluate a Bézier curve $b_2(t; x_0, x_1, x_2)$ at a point t , we would need three line evaluations: $y_0 = b_1(t; x_0, x_1)$, $y_1 = b_1(t; x_1, x_2)$ and their connecting line $b_2(t; x_0, x_1, x_2) = b_1(t; y_0, y_1)$. The result is a quadratic curve in \mathbb{R}^n .

On a Riemannian manifold \mathcal{M} we obtain a Bézier curve by evaluating shortest geodesics $\gamma(t; p, q)$ connecting $p, q \in \mathcal{M}$ instead of line segments.

The implementation for an arbitrary Riemannian manifold is given by the following code and returns the Bézier curve evaluated at t .

```
function bezier(M::AbstractManifold, t, pts::NTuple)
    p = bezier(M, t, pts[1:(end - 1)])
    q = bezier(M, t, pts[2:end])
    return shortest_geodesic(M, p, q, t)
end
function bezier(M::AbstractManifold, t, pts::NTuple{2})
    return shortest_geodesic(M, pts[1], pts[2], t)
end
```

For four points on the sphere given by

$$p_0 = (0 \quad -1 \quad 0)^T, \quad p_1 = \left(-\frac{1}{2} \quad -\frac{1}{\sqrt{2}} \quad -\frac{1}{2}\right)^T, \quad p_2 = \left(-\frac{1}{\sqrt{2}} \quad -\frac{1}{2} \quad \frac{1}{2}\right)^T, \quad p_3 = (-1 \quad 0 \quad 0)^T,$$

and an evaluation of b_3 at $t = \frac{2}{3}$ all shortest geodesics involved in the evaluation are shown in Figure 2. This figure has been adapted from (Bergmann and Gousenbourger, 2018, Figure 9).

5.2 Optimization using Manopt.jl

Now, we consider the generalization of the mean to Riemannian manifolds. The mean of some (Euclidean) data $x_1, \dots, x_N \in \mathbb{R}^n$ can be computed as

$$\hat{x} = \frac{1}{N} \sum_{k=1}^N x_k.$$

One can interpret this formula as the first-order optimality condition of the optimization problem

$$\hat{x} = \arg \min_{y \in \mathbb{R}^n} \sum_{k=1}^N \|x_k - y\|^2.$$

That is, \hat{x} is the point y that minimizes the sum of squared distances. This interpretation can be generalized to manifolds, but usually no closed form for y , like \hat{x} in the Euclidean case, exists. Still, replacing the squared deviation with the squared distance, the gradient can easily be computed to perform a gradient descent algorithm with a suitable line search

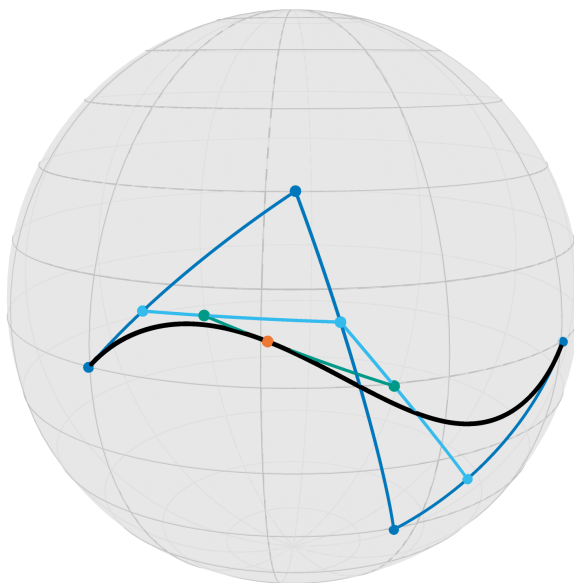


Figure 2: Illustration of the De Casteljau algorithm to evaluate a Bézier curve on the Sphere \mathbb{S}^2 . The initial points and their shortest geodesics (blue) yield three points (cyan) and two points (green) during the recursion, and their connecting geodesic the point on the Bézier curve (orange).

strategy, cf. for example (Absil et al., 2008, Chapter 4). For given points $p_1, \dots, p_N \in \mathcal{M}$ the cost function and the gradient read

$$F(q) = \frac{1}{N} \sum_{k=1}^N d_{\mathcal{M}}^2(q, p_k) \quad \text{and} \quad \text{grad } F(q) = -\frac{1}{2N} \sum_{k=1}^N \log_q p_k.$$

This algorithm `gradient_descent` is implemented in `Manopt.jl`. Furthermore, a library of cost functions, gradients, differentials, adjoint differentials as well as proximal maps is available in the package as well. They are implemented on arbitrary manifolds based only on `ManifoldsBase.jl` and can hence be used to phrase an optimization problem even independent of the manifold. One example that we also require here is the already mentioned gradient of the distance function (squared) `distance(M, p, q)^s` with respect to q , where $s=2$ is the default. This function is called `grad_distance(M, p, q, s)` in `Manopt.jl`.

Note that since `Manopt.jl` is based on the lightweight interface `ManifoldsBase.jl`, we need to load `Manifolds.jl` only to have our manifold of interest available.

```
using Manopt, Manifolds, LinearAlgebra
M = Sphere(2)
N = 100
# generate random points on M
pts = [normalize(randn(3)) for _ in 1:N]
# define the loss function and its gradient
F(M, q) = sum(p -> distance(M, p, q)^2 / 2N, pts)
```

```

gradF(M,q) = sum(p -> grad_distance(M, p, q) / N, pts)
# compute the mean
xMean = gradient_descent(M, F, gradF, pts[1])

```

`Manifolds.jl` itself includes two approaches for computing the weighted mean: gradient descent and on-line repeated geodesic interpolation (Ho et al., 2013). Using these methods, implementations of weighted variance, skewness, kurtosis, and higher moments are also provided.

5.3 Tangent space PCA

Thanks to the high composability of the Julia ecosystem and the design of the `Manifolds.jl` library, it is very easy to compose independent libraries to achieve new functionality. For example, tangent space principal component analysis (PCA) described by Fletcher et al. (2004) can be split into 1) computing the Riemannian center of mass and coordinates of tangent vectors using `Manifolds.jl` and 2) calculation of PCA vectors using `MultivariateStats.jl`. Using a d -dimensional manifold, tangent vectors might be stored in a format different from the d -dimensional vector. The interface `ManifoldsBase.jl` provides `get_coordinates` to obtain a d -dimensional representation and `get_vector` to reconstruct the tangent space format. For example tangent vectors from $T_p\mathbb{S}^2$ are stored as vectors X orthogonal to p (in \mathbb{R}^3) and they have a representation in 2 coordinates. The whole procedure is demonstrated by the following code.

```

using Manifolds, MultivariateStats, LinearAlgebra
M = Sphere(2)
N = 100
# generate random points on M
pts = [normalize(randn(3)) for _ in 1:N]
# compute their mean
m = mean(M, pts)
# compute logarithmic maps of points at their mean
vectors = map(p -> log(M, m, p), pts)
# choose a basis of the tangent space at point m
basis = DefaultOrthonormalBasis()
# compute coordinates of tangent vectors in the selected basis
coords = map(X -> get_coordinates(M, m, X, basis), vectors)
# flatten the array of coordinates to a matrix
coords_red = reduce(hcat, coords)
z = zeros(manifold_dimension(M))
# compute the first principal vector assuming zero mean
model = fit(PCA, coords_red; maxoutdim=1, mean=z)
# get the tangent vector corresponding to the first principal vector
X = get_vector(M, m, reconstruct(model, [1.0]), basis)

```

6. Benchmarks

This section presents and discusses benchmarks performed to compare performance of `Manifolds.jl` to other libraries. Operations on five different manifolds were benchmarked: the Euclidean

manifold \mathbb{R}^3 , the manifold of rotations $\text{SO}(3)$, the manifold of symmetric positive definite matrices $\mathcal{P}(3)$ with the linear affine metric, the power manifold $\mathcal{P}(3)^{128 \times 128}$ encountered in diffusion tensor imaging (Ghosh et al., 2008) and the unit sphere \mathbb{S}^2 . For all manifolds three operations were benchmarked: calculation of the distance d between two points, an inverse retraction retr^{-1} , and a retraction retr . Whenever possible, we compare the same operations for all packages. However, when an operation for a given manifold was not available in all packages, a default was used instead.

6.1 General setup

A computer running Linux Mint 20 Ulyana with Intel(R) Core(TM) i7-9700KF CPU @ 3.60GHz CPU and 32 GB of RAM was used to benchmark all libraries. In particular, no limitations were imposed on the number of threads.

The benchmarking was performed using points generated randomly by `Manifolds.jl`. Each benchmarked operation was performed 10^N times in a loop written in the language native to the library. The number N was chosen to be large enough to ensure that the entire benchmarking loop takes at least one second to reduce the influence of system clock inaccuracy. Results of operations were accumulated in an array, which incurs a small performance penalty but prevents the compiler from optimizing out an otherwise unused computation. Details of benchmarks specific to particular libraries and the setting used are given in the supplementary material.

6.2 Discussion

Figure 3 contains results of performed benchmarks. `Manifolds.jl` (black lines) is the fastest in all three performed function tests (rows) on all manifolds (columns). The results indicate that the Python libraries have a large overhead related to calling C code that performs the actual computation. As a result, all algorithms written in Python that use these operations have limited speed, unless the overhead is small in comparison to the time needed to perform the actual operation, as demonstrated by $\mathcal{P}(3)^{128 \times 128}$ in `pymanopt`. `Manopt` exhibits similar behavior, while `ROPTLIB`, being a native C++ library, does not. `ROPTLIB`'s performance is slower by a factor of 2 than that of `Manifolds.jl`. This is probably due to the more sophisticated memory management and use of specialized linear algebra packages in `Manifolds.jl`.

7. Conclusions

`Manifolds.jl` provides a comprehensive API and set of features for working with points on manifolds. It also offers one of the largest collections of implementations of manifolds. Using this API, `Manopt.jl` provides a library of algorithms for optimization on manifolds. As a result, all manifolds defined with `ManifoldsBase.jl` are compatible with `Manopt.jl` and can directly be used therein.

One prominent advantage of `Manifolds.jl` over similar packages is that, by using Julia, the “two-language-barrier” is overcome while keeping the code concise and expressive. Implementations in `Manifolds.jl` were demonstrated to be superior in performance to those in libraries with interfaces in Python and Matlab and approximately twice as fast as `ROPTLIB`.

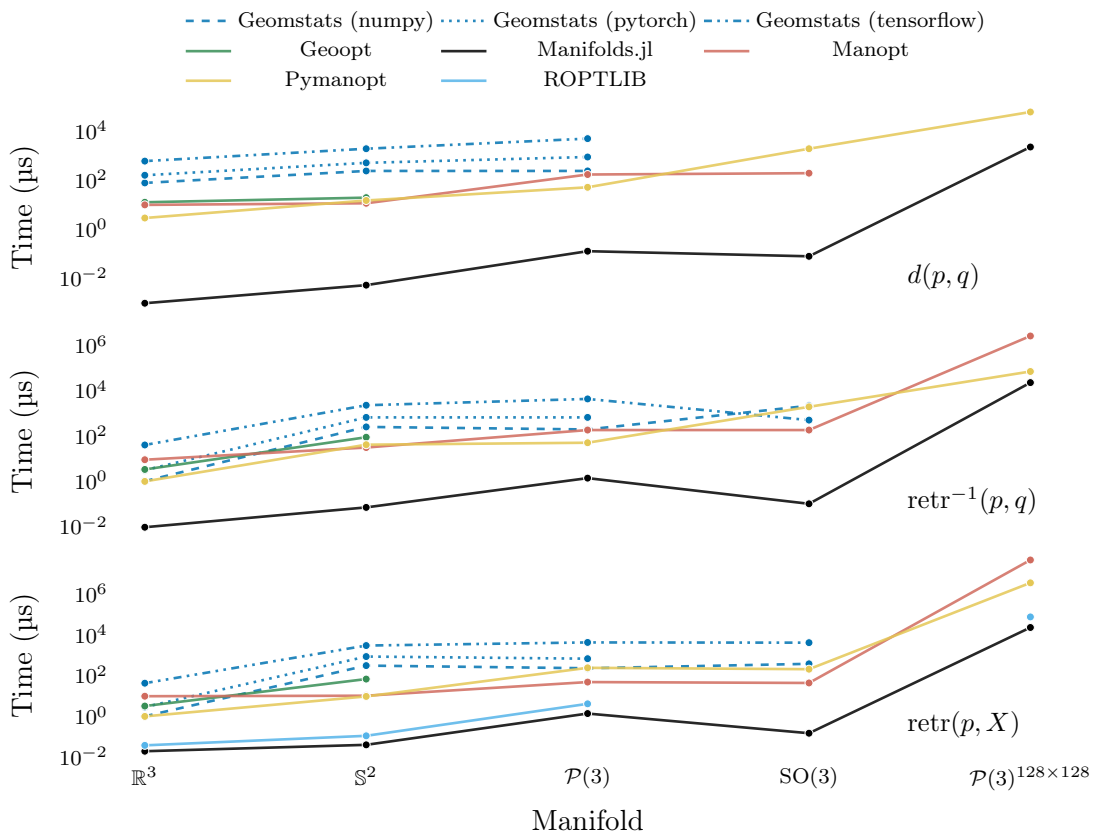


Figure 3: Benchmark of distance (top row), an inverse retraction (middle row) and a retraction (bottom row) on several manifolds (columns) for 6 tested implementations, where Geomstats further features three backends. `Manifolds.jl` (black lines) features both the fastest runtimes as well as the largest variety of available functions. Numerical values of runtimes are given in Table S1.

However, this high performance did not require sacrificing clarity of the implementations themselves or the ease of use of a dynamic programming language.

Future work on `Manifolds.jl` will improve integration of Julia’s automatic differentiation packages, add support for GPU acceleration, and expand the set of available manifolds and operations. Other plans include support for more statistical and machine learning methods.

Acknowledgments

SDA was supported by the National Science Foundation under grant number 1650113. MB and KR were funded by the AGH University of Science and Technology in the year 2021 as a research project No. 16.16.120.773 and by Foundation for Polish Science under grant POIR.04.04.00-00-15E5/18.

References

- P.-A. Absil, R. Mahony, and R. Sepulchre. *Optimization Algorithms on Matrix Manifolds*. Princeton University Press, 2008. doi: 10.1515/9781400830244.
- P.-A. Absil, P.-Y. Gousenbourger, P. Striowski, and B. Wirth. Differentiable piecewise-bézier surfaces on riemannian manifolds. *SIAM Journal on Imaging Sciences*, 9(4):1788–1828, 2016. doi: 10.1137/16M1057978.
- M. Baran. Closest paths in graph drawings under an elastic metric. *International Journal of Applied Mathematics and Computer Science*, 28(2):387–397, 2018. ISSN 1641-876X. doi: 10.2478/amcs-2018-0029.
- M. Bačák. Computing medians and means in hadamard spaces. *SIAM Journal on Optimization*, 24(3):1542–1566, 2014. doi: 10.1137/140953393.
- M. Bačák, R. Bergmann, G. Steidl, and A. Weinmann. A second order non-smooth variational model for restoring manifold-valued images. *SIAM Journal on Scientific Computing*, 38(1):A567–A597, 2016. doi: 10.1137/15M101988X.
- R. Bergmann. MVIRT, a toolbox for manifold-valued image restoration. In *IEEE International Conference on Image Processing, IEEE ICIP 2017, Beijing, China, September 17–20, 2017*, 2017. doi: 10.1109/ICIP.2017.8296271.
- R. Bergmann. Manopt.jl. optimization on manifolds in Julia, 2019. URL <https://manoptjl.org/>. doi: 10.5281/zenodo.4290905.
- R. Bergmann and P.-Y. Gousenbourger. A variational model for data fitting on manifolds by minimizing the acceleration of a Bézier curve. *Frontiers in Applied Mathematics and Statistics*, 2018. doi: 10.3389/fams.2018.00059.
- R. Bergmann, J. Persch, and G. Steidl. A parallel douglas rachford algorithm for minimizing rof-like functionals on images with values in symmetric hadamard manifolds. *SIAM Journal on Imaging Sciences*, 9(4):901–937, 2016. doi: 10.1137/15M1052858.

- R. Bergmann, J. H. Fitschen, J. Persch, and G. Steidl. Priors with coupled first and second order differences for manifold-valued image processing. *Journal of Mathematical Imaging and Vision*, 60(9):1459–1481, 2018. ISSN 0924-9907. doi: 10.1007/s10851-018-0840-y.
- J. Bezanson, A. Edelman, S. Karpinski, and V. Shah. Julia: A Fresh Approach to Numerical Computing. *SIAM Review*, 59(1):65–98, Jan. 2017. ISSN 0036-1445. doi: 10.1137/141000671. URL <https://epubs.siam.org/doi/10.1137/141000671>.
- N. Boumal, B. Mishra, P.-A. Absil, and R. Sepulchre. Manopt, a Matlab toolbox for optimization on manifolds. *Journal of Machine Learning Research*, 15(42):1455–1459, 2014. URL <https://www.manopt.org>.
- L. Chen, V. P. Singh, S. Guo, B. Fang, and P. Liu. A new method for identification of flood seasons using directional statistics. *Hydrological Sciences Journal*, 58(1):28–40, Jan. 2013. ISSN 0262-6667. doi: 10.1080/02626667.2012.743661.
- L. M. Cruz-Orive, H. Hoppeler, O. Mathieu, and E. R. Weibel. Stereological Analysis of Anisotropic Structures Using Directional Statistics. *Journal of the Royal Statistical Society: Series C (Applied Statistics)*, 34(1):14–32, 1985. ISSN 1467-9876. doi: 10.2307/2347881.
- M. P. a. do Carmo. *Riemannian Geometry*. Mathematics: Theory & Applications. Birkhäuser Boston, Inc., Boston, MA, 1992. ISBN 0-8176-3490-8.
- I. L. Dryden, A. Koloydenko, and D. Zhou. Non-Euclidean statistics for covariance matrices, with applications to diffusion tensor imaging. *Annals of Applied Statistics*, 3(3):1102–1123, Sept. 2009. ISSN 1932-6157, 1941-7330. doi: 10.1214/09-AOAS249. Publisher: Institute of Mathematical Statistics.
- P. Fletcher, C. Lu, S. Pizer, and S. Joshi. Principal geodesic analysis for the study of nonlinear statistics of shape. *IEEE Transactions on Medical Imaging*, 23(8):995–1005, Aug. 2004. ISSN 0278-0062. doi: 10.1109/TMI.2004.831793.
- A. Ghosh, M. Descoteaux, and R. Deriche. Riemannian framework for estimating symmetric positive definite 4th order diffusion tensors. *Medical image computing and computer-assisted intervention: MICCAI ... International Conference on Medical Image Computing and Computer-Assisted Intervention*, 11(Pt 1):858–865, 2008. doi: 10.1007/978-3-540-85988-8_102.
- P.-Y. Gousenbourger, E. Massart, and P.-A. Absil. Data fitting on manifolds with composite bézier-like curves and blended cubic splines. *Journal of Mathematical Imaging and Vision*, 61(5):645–671, 2018. doi: 10.1007/s10851-018-0865-2.
- U. Grenander and M. I. Miller. Computational anatomy: an emerging discipline. *Quarterly of Applied Mathematics*, 56(4):617–694, 1998. ISSN 0033-569X, 1552-4485. doi: 10.1090/qam/1668732.
- K. Grove and H. Karcher. How to conjugate c^1 -close group actions. *Mathematische Zeitschrift*, 132:11–20, 1973. ISSN 0025-5874. doi: 10.1007/BF01214029.

- J. Ho, G. Cheng, H. Salehian, and B. Vemuri. Recursive karcher expectation estimators and geometric law of large numbers. In C. M. Carvalho and P. Ravikumar, editors, *Proceedings of the Sixteenth International Conference on Artificial Intelligence and Statistics*, volume 31 of *Proceedings of Machine Learning Research*, pages 325–332, Scottsdale, Arizona, USA, 29 Apr–01 May 2013. PMLR. URL <http://proceedings.mlr.press/v31/ho13a.html>.
- W. Huang, P.-A. Absil, K. A. Gallivan, and P. Hand. ROPTLIB: An Object-Oriented C++ Library for Optimization on Riemannian Manifolds. *ACM Transactions on Mathematical Software*, 44(4):43:1–43:21, July 2018. ISSN 0098-3500. doi: 10.1145/3218822.
- H. Karcher. Riemannian center of mass and mollifier smoothing. *Communications on Pure and Applied Mathematics*, 30(5):509–541, 1977. doi: 10.1002/cpa.3160300502.
- M. Kochurov, R. Karimov, and S. Kozlukov. Geopt: Riemannian Optimization in PyTorch. *arXiv:2005.02819 [cs]*, July 2020. URL <http://arxiv.org/abs/2005.02819>.
- L. Kühnel and S. Sommer. Computational Anatomy in Theano. In M. J. Cardoso, T. Arbel, E. Ferrante, X. Pennec, A. V. Dalca, S. Parisot, S. Joshi, N. K. Batmanghelich, A. Sotiras, M. Nielsen, M. R. Sabuncu, T. Fletcher, L. Shen, S. Durrleman, and S. Sommer, editors, *Graphs in Biomedical Image Analysis, Computational Anatomy and Imaging Genetics*, Lecture Notes in Computer Science, pages 164–176, Cham, 2017. Springer International Publishing. ISBN 978-3-319-67675-3. doi: 10.1007/978-3-319-67675-3_15.
- J. Marins, X. Yun, E. Bachmann, R. McGhee, and M. Zyda. An extended Kalman filter for quaternion-based orientation estimation using MARG sensors. In *Proceedings 2001 IEEE/RSJ International Conference on Intelligent Robots and Systems. Expanding the Societal Role of Robotics in the the Next Millennium (Cat. No.01CH37180)*, volume 4, pages 2003–2011 vol.4, Oct. 2001. doi: 10.1109/IROS.2001.976367.
- M. Meghwanshi, P. Jawanpuria, A. Kunchukuttan, H. Kasai, and B. Mishra. McTorch, a manifold optimization library for deep learning. *arXiv:1810.01811 [cs, stat]*, Oct. 2018. URL <http://arxiv.org/abs/1810.01811>.
- M. I. Miller. Computational anatomy: shape, growth, and atrophy comparison via diffeomorphisms. *NeuroImage*, 23 Suppl 1:S19–33, 2004. ISSN 1053-8119. doi: 10.1016/j.neuroimage.2004.07.021.
- N. Miolane, N. Guigui, A. L. Brigant, J. Mathe, B. Hou, Y. Thanwerdas, S. Heyder, O. Peltre, N. Koep, H. Zaatiti, H. Hajri, Y. Cabanes, T. Gerald, P. Chauchat, C. Shewmake, D. Brooks, B. Kainz, C. Donnat, S. Holmes, and X. Pennec. Geomstats: A Python package for Riemannian geometry in machine learning. *Journal of Machine Learning Research*, 21(223):1–9, 2020. URL <http://jmlr.org/papers/v21/19-027.html>.
- X. Pennec, S. Sommer, and T. Fletcher, editors. *Riemannian Geometric Statistics in Medical Image Analysis*. Academic Press, San Diego, 1st edition edition, Sept. 2019. ISBN 978-0-12-814725-2.

- K. Rzecki and M. Baran. Application of elastic shape analysis to user authentication and identification. *IEEE Transactions on Emerging Topics in Computing*, pages 1–1, 2021. doi: 10.1109/TETC.2021.3074242.
- A. Srivastava, E. Klassen, S. H. Joshi, and I. H. Jermyn. Shape Analysis of Elastic Curves in Euclidean Spaces. *IEEE Transactions on Pattern Analysis and Machine Intelligence*, 33(7):1415–1428, July 2011. ISSN 0162-8828. doi: 10.1109/TPAMI.2010.184.
- J. Townsend, N. Koep, and S. Weichwald. Pymanopt: A Python Toolbox for Optimization on Manifolds using Automatic Differentiation. *Journal of Machine Learning Research*, 17(137):1–5, 2016. ISSN 1533-7928. URL <http://jmlr.org/papers/v17/16-177.html>.
- M. Tulik, D. Kabat, M. Baran, R. A. Kycia, and Z. Tabor. Use of statistical approaches to improve the quality control of the dose delivery in radiotherapy. *Physics in Medicine & Biology*, 64(14):145018, 2019. ISSN 0031-9155. doi: 10.1088/1361-6560/ab25ab. URL <http://iopscience.iop.org/10.1088/1361-6560/ab25ab>.
- P. Turaga, A. Veeraraghavan, A. Srivastava, and R. Chellappa. Statistical Computations on Grassmann and Stiefel Manifolds for Image and Video-Based Recognition. *IEEE Transactions on Pattern Analysis and Machine Intelligence*, 33(11):2273–2286, Nov. 2011. ISSN 1939-3539. doi: 10.1109/TPAMI.2011.52.

Supplementary – Library-specific details

For `Manifolds.jl`, version 0.5.2² of the library and `ManifoldsBase.jl` version 0.11.4 was used.

- \mathbb{S}^2 : `Sphere(2)`
- \mathbb{R}^3 : `Euclidean(3)`
- $\mathcal{P}(3)$: `SymmetricPositiveDefinite(3)`
- $\mathcal{P}(3)^{128 \times 128}$:
`PowerManifold(SymmetricPositiveDefinite(3), ArrayPowerRepresentation(), 128, 128)`
- $\text{SO}(3)$: `Rotations(3)`

For \mathbb{S}^2 , $\mathcal{P}(3)$, \mathbb{R}^3 , and $\text{SO}(3)$, statically sized arrays were used to represent points and vectors. For $\mathcal{P}(3)^{128 \times 128}$, the array type from `HybridArrays.jl`³ version 0.3.8, was used.

All Python libraries were tested with Python version 3.7.9.final.0 (64 bit).

Geomstats version 2.2.2 was used with Numpy 1.20.3, PyTorch 1.6.0, and Tensorflow 2.5.0. The following commands were used to construct manifolds:

- \mathbb{S}^2 : `hypersphere.HypersphereMetric(2)`
- \mathbb{R}^3 : `euclidean.EuclideanMetric(3)`
- $\mathcal{P}(3)$: `spd_matrices.SPDMetricAffine(3, 1)`
- $\mathcal{P}(3)^{128 \times 128}$ was not available in Geomstats
- $\text{SO}(3)$: `special_orthogonal.SpecialOrthogonal(3)`

All manifolds were taken from the `geomstats.geometry` path (omitted in the list above).

Geoopt version 0.3.1 was benchmarked. The following commands were used to construct manifolds:

- \mathbb{S}^2 : `geoopt.manifolds.Sphere(torch.ones([3, 3]))`
- \mathbb{R}^3 : `geoopt.manifolds.Euclidean(1)`

Other tested manifolds are not available in Geoopt.

Manopt version 6.0.0 (released on May 19, 2020) was used with Matlab version R2020a Update 5 (released on August 6, 2020). The following commands were used to construct manifolds:

- \mathbb{S}^2 : `spherefactory(3)`
- \mathbb{R}^3 : `euclideanfactory(3)`
- $\mathcal{P}(3)$: `sympositivedefinitefactory(3)`

2. The manuscript features a slightly newer version, which has the same benchmark properties

3. see <https://github.com/mateuszbaran/HybridArrays.jl>

- $\mathcal{P}(3)^{128 \times 128}$: `powermanifold(sympositivedefinitefactory(3), 128*128)`
- $\text{SO}(3)$: `rotationsfactory(3)`

Pymanopt version 0.2.5 was used. The following commands were used to construct manifolds:

- \mathbb{S}^2 : `Sphere(3)`
- \mathbb{R}^3 : `euclidean.Euclidean(3)`
- $\mathcal{P}(3)$: `PositiveDefinite(3)`
- $\mathcal{P}(3)^{128 \times 128}$: `PositiveDefinite(3, 128 * 128), 128*128)`
- $\text{SO}(3)$: `rotations.Rotations(3)`

All manifolds were taken from the `pymanopt.manifolds` path (omitted above).

ROPTLIB version 0.8 (released on August 11, 2020) was used, compiled using GCC version 9.3.0 using the provided makefile. The following commands were used to construct manifolds:

- \mathbb{S}^2 : `Sphere(3)`
- \mathbb{R}^3 : `Euclidean(3, "double")`
- $\mathcal{P}(3)$: `SPDManifold(3)`
- $\mathcal{P}(3)^{128 \times 128}$: `ProductManifold prodMani(1, &spdMani, 128 * 128);`, where the variable `spdMani` was defined as `SPDManifold spdMani(3);`
- $\text{SO}(3)$ is not directly implemented (the manual suggests using a special case of Stiefel instead) and was thus not tested

The tested version of ROPTLIB does not provide inverse retractions, and distance calculation can only be performed as a norm of a tangent vector and were excluded as well.

The resulting times are reported in Table 3.

Table 3: Benchmarks of selected functions in related libraries. All times are given in microseconds. n/d indicates that the operation is not available. The manifold $\text{SO}(3)$ was not tested with ROPTLIB because it does not offer the same metric as other libraries.

Manifold	Function	Geomstats with			Geoopt	Manifolds.jl	Manopt	Pymanopt	ROPTLIB
		numpy	pytorch	tensorflow					
\mathbb{R}^3	d	$6.6 \cdot 10^1$	$1.7 \cdot 10^2$	$3.7 \cdot 10^2$	$9.6 \cdot 10^0$	$8.3 \cdot 10^{-4}$	$1.0 \cdot 10^1$	$3.7 \cdot 10^0$	n/d
	retr^{-1}	$9.9 \cdot 10^{-1}$	$3.1 \cdot 10^0$	$1.5 \cdot 10^1$	$3.2 \cdot 10^0$	$8.0 \cdot 10^{-3}$	$8.0 \cdot 10^0$	$1.0 \cdot 10^0$	n/d
	retr	$9.9 \cdot 10^{-1}$	$3.0 \cdot 10^0$	$1.7 \cdot 10^1$	$3.1 \cdot 10^0$	$1.7 \cdot 10^{-2}$	$8.6 \cdot 10^0$	$1.0 \cdot 10^0$	$3.3 \cdot 10^{-2}$
$\text{SO}(3)$	d	n/d	n/d	n/d	n/d	$5.5 \cdot 10^{-2}$	$1.7 \cdot 10^2$	$1.7 \cdot 10^3$	excl
	retr^{-1}	$1.9 \cdot 10^3$	n/d	$1.6 \cdot 10^2$	n/d	$6.4 \cdot 10^{-2}$	$1.6 \cdot 10^2$	$1.8 \cdot 10^3$	excl
	retr	$3.4 \cdot 10^2$	n/d	$1.9 \cdot 10^3$	n/d	$1.0 \cdot 10^{-1}$	$3.8 \cdot 10^1$	$1.8 \cdot 10^2$	excl
$\mathcal{P}(3)$	d	$2.1 \cdot 10^2$	$1.0 \cdot 10^3$	$2.5 \cdot 10^3$	n/d	$2.0 \cdot 10^0$	$1.5 \cdot 10^2$	$4.5 \cdot 10^1$	n/d
	retr^{-1}	$1.7 \cdot 10^2$	$7.2 \cdot 10^2$	$2.2 \cdot 10^3$	n/d	$1.2 \cdot 10^0$	$1.6 \cdot 10^2$	$4.4 \cdot 10^1$	n/d
	retr	$2.0 \cdot 10^2$	$7.5 \cdot 10^2$	$2.2 \cdot 10^3$	n/d	$1.2 \cdot 10^0$	$4.2 \cdot 10^1$	$2.1 \cdot 10^2$	$3.6 \cdot 10^0$
Power $\mathcal{P}(3)$	d	n/d	n/d	n/d	n/d	$3.0 \cdot 10^4$	n/d	$7.1 \cdot 10^4$	n/d
	retr^{-1}	n/d	n/d	n/d	n/d	$2.0 \cdot 10^4$	$2.2 \cdot 10^6$	$8.0 \cdot 10^4$	n/d
	retr	n/d	n/d	n/d	n/d	$2.0 \cdot 10^4$	$4.3 \cdot 10^7$	$3.1 \cdot 10^6$	$7.4 \cdot 10^4$
\mathbb{S}^2	d	$2.1 \cdot 10^2$	$5.4 \cdot 10^2$	$1.2 \cdot 10^3$	$1.9 \cdot 10^1$	$4.6 \cdot 10^{-3}$	$1.1 \cdot 10^1$	$1.4 \cdot 10^1$	n/d
	retr^{-1}	$4.2 \cdot 10^2$	$9.2 \cdot 10^2$	$2.0 \cdot 10^3$	$8.3 \cdot 10^1$	$5.8 \cdot 10^{-2}$	$2.8 \cdot 10^1$	$3.8 \cdot 10^1$	n/d
	retr	$2.9 \cdot 10^2$	$8.4 \cdot 10^2$	$4.6 \cdot 10^3$	$6.4 \cdot 10^1$	$3.6 \cdot 10^{-2}$	$9.3 \cdot 10^0$	$8.7 \cdot 10^0$	$1.0 \cdot 10^{-1}$